A Linear Actuation of Polymeric Nanofibrous Bundle for Artificial Muscles

Bon Kang Gu,[†] Yahya A. Ismail,[†] Geoffrey M. Spinks,[‡] Sun I. Kim,[†] Insuk So,[§] and Seon Jeong Kim*,[†]

Creative Research Center for Bio-Artificial Muscle, Department of Biomedical Engineering, Hanyang University, Seoul, Korea, Intelligent Polymer Research Institute, University of Wollongong, Wollongong, Australia, and Department of Physiology, Seoul National University, Seoul, Korea

Received September 3, 2008. Revised Manuscript Received December 3, 2008

Artificial muscle fiber mimicking myofibril is fabricated using electrospun nanofibers of high strength polyurethane followed by controlled in situ chemical polymerization with aniline. The resulting polyurethane(PU)/polyaniline(PANi) hybrid nanofibrous bundle consisting individual nanofibers of about 900 nm diameter responds to an electrical stimuli producing a linear actuation strain as high as 1.65% at an applied stress of 1.03 MPa in 1 M methane sulfonic acid (MSA), the highest strain produced in the nanofibers templated PANi. The hybrid nanofibrous bundle shows an electrical conductivity of about 0.5 S/cm and the electroactivity is imparted by PANi. The biomimetic artificial nanofibrous bundle shows work per cycle (W.C.) efficiency of above 75% for the electrochemical actuation even beyond 100 cycles. The PU/PANi hybrid nanofibrous bundle could be stably actuated without significant creep up to an applied load of 11 mN (2.263 Mpa) beyond which significant creep behavior appears.

Introduction

Emulating the function of natural muscle remains as a significant challenge to the scientific community. The primary unit of any biological systems responsible for mechanical motion is the muscle fiber. The large actuation strains and fast response from muscle generate sufficient mechanical power to enable swimming, running, climbing, and flying type locomotion in organisms covering several orders of magnitude in size. The performance of natural muscle derives from its detailed nanostructure and efforts have been made to emulate these structures in artificial systems.[1−3] In human muscles, the largest functional unit of contractile skeletal muscle is the myofibril. Myofibrillar diameter is about 1 μm, and thousands of myofibrils are packed in a parallel bundle to form a single muscle fiber. Groups of muscle fibers are surrounded by a connective tissue sheath and arranged in bundles called fascicles. These fascicles are also bundled together, surrounded by more connective tissue to form the whole muscle.[4] The fiber bundles allow fast reaction speeds because diffusion distances (and times) are small for the molecular species responsible for muscle contraction.

For biomimicking the functional unit of a skeletal muscle fiber in an artificial muscle system, we employed electrospinning of a polymer solution.[5−7] Using a cone type electrode, we formed polymer nanofiber bundles having a uniform shape and parallel orientation that resembled myofibrils. Conventional electrospinning is a simple technique that converts a polymer solution into nanofibers having a uniform shape but with a random orientation.[8] Recently, however, several research groups have introduced techniques aimed at controlling the shape and alignment of nanofibers by using a modified electric field.[9−11] The alignment of nanofiber is very important to actuator function, as it maximizes the mechanical work output.

In this work, we have chosen a conducting polymer as the artificial muscle material. Conducting polymers are receiving considerable attention for fabricating lightweight actuators because they can be actuated using low operational voltage and resulting in a fairly high strain and strain rate.[12,13] Among these materials, polyaniline (PANi) is favorable because of its environmental stability and ease of synthesis. Recently, we developed a hydrogel assisted PANi microfiber for artificial muscle.[14] Moreover, Spinks et al. have reported highly drawn PANi fibers reinforced with carbon nanotube

* To whom correspondence should be addressed. E-mail:sjk@hanyang.ac.kr. Tel:82-2-2220-2321. Fax:82-2-2291-2320.
[†] Hanyang University.
[‡] University of Wollongong.
[§] Seoul National University.

(1) Madden, J. D. *Science* **2007**, *318*, 1094.
(2) Feinberg, A. W.; Feigel, A.; Shevkoplyas, S. S.; Sheehy, S.; Whitesides, G. M.; Parker, K. K. *Science* **2007**, *317*, 366.
(3) Robinson, D. W.; Pratt, J. E.; Paluska, D. J.; Pratt, G. A. In *Proceedings of 1999 IEEE/ASME International Conference on Advanced Intelligent Mechatronics*; IEEE: Piscataway, NJ, 1999; pp 561−568.
(4) Thibodeau, G. A.; Patton, K. T. In *Anatomy & Physiology*, 5th ed.; Mosby: St. Louis, MO, 2003; Chapter 10.
(5) Dzenis, Y. *Science* **2004**, *304*, 1917.
(6) Reneker, D. H.; Chun, I. *Nanotechnology* **1996**, *7*, 216.
(7) Greiner, A.; Wendrff, J. H. *Angew. Chem.* **2007**, *46*, 5670.
(8) Reneker, D. H.; Doshi, J. *J. Electrost.* **1995**, *35*, 151.
(9) Li, D.; Wang, Y.; Xia, Y. *Nano Lett.* **2003**, *3*, 1167.
(10) Teo, W. E.; Ramakrishna, S. *Nanotechnology* **2005**, *16*, 1878.
(11) Shin, M. K.; Kim, S. I.; Kim, S. J. *Appl. Phys. Lett.* **2006**, *88*, 223109.
(12) Smela, E.; Lu, W.; Mattes, B. R. *Synth. Met.* **2005**, *151*, 25.
(13) Smela, E. *Adv. Mater.* **2003**, *15*, 481.
(14) Ismail, Y. A.; Shin, S. R.; Shin, K. M.; Yoon, S. G.; Shon, K. W.; Kim, S. I.; Kim, S. J. *Sens. Actuators, B* **2008**, *129*, 834.

10.1021/cm802377d CCC: $40.75
Published on Web 01/06/2009

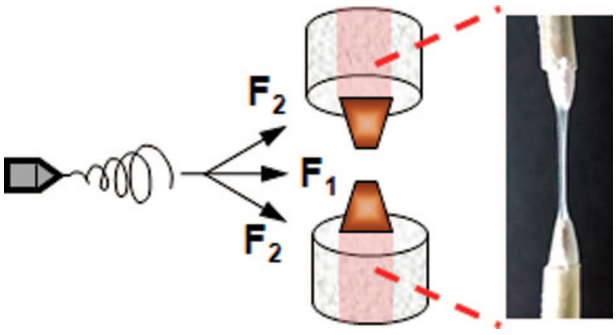

Figure 1. Schematic diagram of the modified electrospinning set up for preparing electrospun nanofibrous bundle. The actual image of the right photograph is suspended nanofiber bundle between parallel conical shaped electrodes. The arrows ($\mathbf{F}_1$, $\mathbf{F}_2$) indicate the direction of electrostatic force.

(CNT) for high strength artificial muscles.[15] Although, many researchers have reported on PANi actuators based on microfibers and films,[16,17] fabrication of an efficient PANi actuator based on aligned nanofibers has yet to be realized.

Because direct electrospinning of PANi to produce highly conducting material is difficult, we chose a templating technique. Electrospun aligned nanofiber bundles were first prepared using polyurethane (PU). In the second phase of fabrication we imparted the electroactivity and conductivity to the nanofibrous bundle through controlled in situ chemical polymerization with aniline. PU was chosen to give a flexible nanofibrous bundle because of its rubbery nature,[18] which would not greatly restrict the actuation of the PANi coating. Herein, we designed such a system mimicking the myofibrils through engineering the nanostructured PU and PANi, and investigated its actuation performance.

Experimental Section

PU (Hosung Chemax Co., Korea) with an average molecular weight of 1.2×10^5 g/mol, ammonium persulfate, hydrochloric acid, methane sulfonic acid (MSA), and chloroform (all Aldrich, USA) were used as received. Aniline (Aldrich, USA) was distilled prior to use. A 10 wt% solution of PU in chloroform was used for electrospinning to produce the nanofibrous bundle.

A schematic drawing of the experimental set up used for the fabrication of nanofibrous bundle is shown in Figure 1. The syringe tip was given a +7 kV charge, the collector (conical electrodes) a −5 kV charge. The distance between the syringe tip and the collector was 13 cm. The polymer solution was loaded into a glass syringe equipped with a 23 gauge stainless steel needle. A syringe pump located in a horizontal mount controlled the flow rate of the polymer solution. The solution feed flow rate used was 4 μL/min. The gap between the two conical shape electrodes was fixed at 1.5 cm to produce uniform and parallel nanofibrous bundle.

Electroactivity for the PU nanofibrous bundles were imparted by polyaniline through an in situ chemical polymerization method similar to the one which we developed recently.[14] In the typical procedure, the nanofibrous PU bundle was suspended in aniline solution in 1 M HCl and ammonium persulphate was used as the catalyst for polymerization reaction which was continued for 24 h. The singly coated PU/PANi nanofibrous bundle was again subject to in situ polymerization with aniline in order to get the PU/PANi hybrid nanofibrous bundle.

The surface morphology and diameter of the hybrid nanofibrous bundle were examined using field emission scanning electron microscopy (FE-SEM, Model S4800, Hitachi, Japan) at an accelerator voltage of 15 kV.

FT-IR spectra of the nanofibrous bundle were carried out by using ATI Mattson, Infinity Series FT-IR Spectrometer (Infinity Gold FT-IR 60AR, USA). The two-point probe room-temperature electrical conductivity was measured using Keithley electrometer (model 2400, USA). The conductivity was calculated from the $I-V$ curve using the equation, $\sigma = I/V \times l/A$, where I is the current, V is the voltage, l is the length, and A is the cross-sectional area of the nanofibrous bundle.

Electrochemical actuation of the nanofibrous bundle was carried out using an Aurora Scientific Inc. (Canada) dual-mode muscle lever arm system with an attached cyclic voltammograph (model CHI 627B electrochemical analyzer). One end of the nanofibrous bundle was fixed at the tip of the muscle lever arm using silicon glue. The other and was clamped and connected to the electrochemical assembly using thin platinum wire. The experiment was carried out using three-electrode electrochemical assembly with the nanofibrous bundle as the working electrode, Ag/AgCl as the reference electrode and a Pt mesh as the counter electrode. 1 M MSA was used as the electrolyte. The potential was cycled between −0.2 and 0.8 V. Prior to the application of cyclic potential the nanofibrous bundle was equilibrated in 1 M MSA for 1 h under applied load of 1.028 MPa. The cyclic voltammogrms of the nanofibrous bundle was recorded under the same experimental setup as described for electrochemical actuation. Mechanical property was measured using Thermo Mechanical Analyzer (Seiko Exstar 6000, Japan).

Results and Discussion

A schematic drawing of the experimental apparatus used for electrospinning is shown in Figure 1. The electrospinning apparatus consists of positive and negative high voltage power supplies, a syringe pump, and conical-shaped copper electrodes for making nanofibrous bundles. The two conical-shaped electrodes placed in line with a gap between them were used as counter electrodes to guide the electrospinning jet and to deposit the nanofibers. The conical-shaped electrodes were used as they were easy to design and have smaller surface area along the conical edge. As can be seen from Figure 1, an insulation tube (silicon) was used to shield unnecessary charges around the conical shaped electrodes, so that the area of the deposition point of the nanofibers was highly reduced. The charged nanofibers experienced two different electrostatic forces. The first electrostatic force ($\mathbf{F}_1$) was in the same direction as the applied electric field, and the second electrostatic force ($\mathbf{F}_2$) was from the Coulombic interactions between the airborne nanofibers and the charges on the surface of the parallel conical shaped electrodes (see the direction of arrows in Figure 1). These electrostatic forces controlled the orientation of the fibers using the split electric field of the parallel conical shaped electrodes.[19] Coulombic interaction between the fiber ends and the electrodes should stretch the nanofiber across the gap to have it positioned

(15) Spinks, G. M.; Mottaghitalab, V.; Bahrami-Samani, M.; Whitten, P. G.; Wallace, G. G. *Adv. Mater.* **2006**, *18*, 637.
(16) Lu, W.; Norris, I. D.; Mattes, B. R. *Aust. J. Chem.* **2005**, *58*, 263.
(17) Baker, C. O.; Shedd, B.; Innis, P. C.; Whitten, P. G.; Spinks, G. M.; Wallace, G. G.; Kaner, R. B. *Adv. Mater.* **2008**, *20*, 155.
(18) Zilg, C.; Thomann, R.; Mulhaupt, R.; Finter, J. *Adv. Mater.* **1999**, *11*, 9.
(19) Gu, B. K.; Shin, M. K.; Shon, K. W.; Kim, S. I.; Kim, S. J.; Kim, S. K.; Lee, H.; Park, J. S. *Appl. Phys. Lett.* **2007**, *90*, 263902.

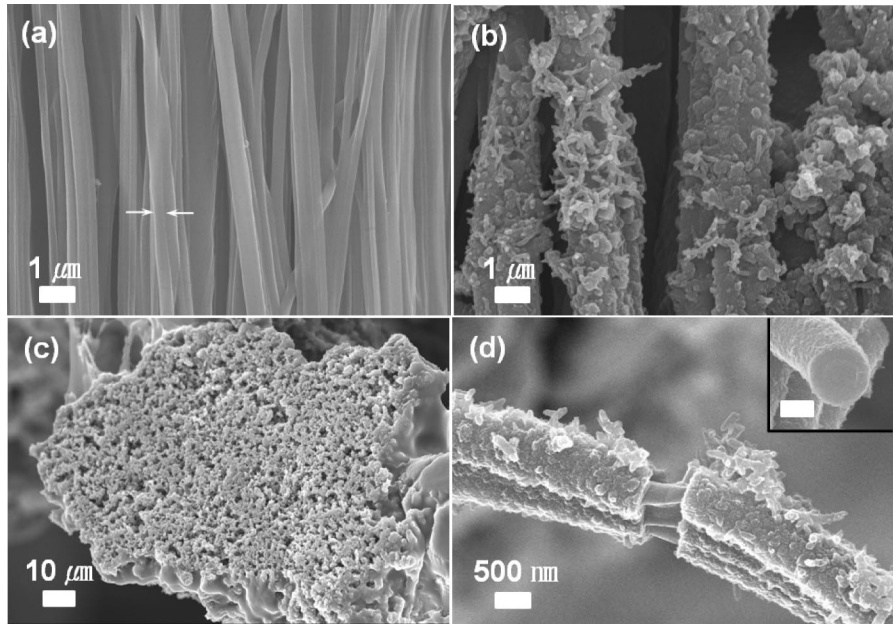

Figure 2. FE-SEM images of PU/PANi hybrid nanofibrous bundles. (a) Pure PU electrospun nanofibers in the bundle showing highly aligned individual nanofibers (arrows indicate a single nanofiber); (b) PU/PANi hybrid nanofibrous bundle after in situ polymerization; (c) cross-sectional SEM image of the PU/PANi hybrid nanofibrous bundle; (d) SEM image of PU/PANi hybrid nanofibrous bundle showing complete coating of each individual PU nanofiber with nanostructured PANi. The inset shows the cross-sectional SEM image of a single PU/PANi hybrid nanofiber (scale bar of inset image: 500 nm).

perpendicular to the edge of the electrode, and resulting in a highly aligned nanofibrous bundle.

Figure 2 shows the field emission scanning electron microscopy (FE-SEM) images of pure PU and PU/PANi hybrid nanofibrous bundles. As can be seen from Figure 2a, the FE-SEM images of pure PU nanofibrous bundle shows well aligned individual nanofibers. After the in situ polymerization with aniline, the resulting PU/PANi hybrid nanofibrous bundle has a complete coating of PANi on the surface of the individual PU nanofibers (Figure 2b). Figure 2c shows the cross-sectional FE-SEM image of the PU/PANi hybrid nanofibrous bundle having an average diameter of about 90 μm. From Figure 2c and using Meta Morph computer programming (Molecular Devices, USA), we assessed the total cross-sectional area (provided by individual hybrid nanofibers) of the bundle to be 4862 μm^2 and total area provided by the voids to be 2378 μm^2. The high porosity in the bundle structure is likely to assist in efficient diffusion of ions from the electrolyte to the PANi and produce higher actuation. The complete coating of PANi on individual PU nanofibers in the hybrid bundle is also illustrated in the FE-SEM image shown in Figure 2(d). It was observed that the individual hybrid nanofibers in the bundles have a diameter of about 900 nm, which is comparable with the diameter of a single myofibril. The average diameter of PU nanofiber was about 400 nm and the thickness of PANi coating was about 250 nm. The inset of Figure 2d shows the cross-sectional images of individual nanofibers from which the thickness of the PANi coatings was estimated. The volume fraction of PANi in the hybrid structure is ~80%. It can also be seen that nanostructured PANi wires were grown on the surface of individual nanofibers giving a high surface area to volume ratio.

Fourier transform infrared spectra (FT-IR) of pure PU and PU/PANi hybrid nanofibrous bundles showed peaks corresponding to the characteristic absorptions of PU and PANi without any evidence of additional peaks (see Figure S1 in Supporting Information). To assess the potential of the PU/PANi hybrid nanofibrous bundle as electrochemical actuators and capacitors, their electroactivity was investigated in aqueous methane sulfonic acid (MSA) by cyclic voltammetry (CV) and the result is given in Figure 3a. The shape of cyclic voltammogram indicated that high electroactivity was produced by the in situ polymerization method.

$I-V$ plots of the PU and PU/PANi hybrid nanofibrous bundle are shown in Figure 3b. The hybrid nanofibrous bundle showed reasonably high electrical conductivity of 0.5 S/cm which was considerably higher than pure PU nanofibrous bundle (1.76×10^{-8} S/cm). The PU/PANi hybrid material conductivity was comparable to other doped polyaniline films.[20]

The high porosity observed in the hybrid nanofibrous bundle allowed the efficient diffusion of ions and the high surface area provided by the individual nanofibers in the bundles along with the growth of nanostructured polyaniline wires grown on the surface of the highly aligned bundles were responsible for the higher electrochemical actuation. Moreover, the cylindrical form of individual nanofibers could provide the perfect utilization of ion diffusion throughout the curvature, which also contributed toward higher actuation. We calculated the diffusion coefficient from CV data obtained at different scan rates using the Randles−Sevcik equation[21]

(20) Xi, B.; Truoung, V.-T.; Mottaghitalab, V.; Whitten, P. G.; Spinks, G. M.; Wallace, G. G. *Smart Mater. Struct.* **2007**, *16*, 1549.
(21) Wang, J. *Analytical Electrochemistry*, 2nd ed.; Wiley-VCH: Weinheim, Germany, 2000.

$$i_p = 269n^{3/2}AD^{1/2}v^{1/2}C^b \quad (1)$$

where D is diffusion coefficient, i_p is peak current, n is number of electron transferred, A is the area of the bundle, v is scan rate, and C^b is concentration. Figure 3c shows the variation of peak current with square root of scan rate. The slope of the line is proportional to the diffusion coefficient. The diffusion coefficient is found to be of the order of 2.3 $\times$ 10^{-4} sec/cm^2. (see Figure S2 in the Supporting Information).

The electrochemical actuation profile of the hybrid nanofibrous bundles in 1 M MSA is presented in Figure 4a. The PU/PANi hybrid nanofibrous bundle responded to the electrical stimulus resulting in an initial linear strain of 1.6% at an applied stress of 1.03 MPa. The active PANi material expands upon oxidation because of the transformation of leucoemeraldine to emeraldine salt with associated anion insertion. Further oxidation to pernigraniline resulted in contraction that was due to the expulsion of cations, which

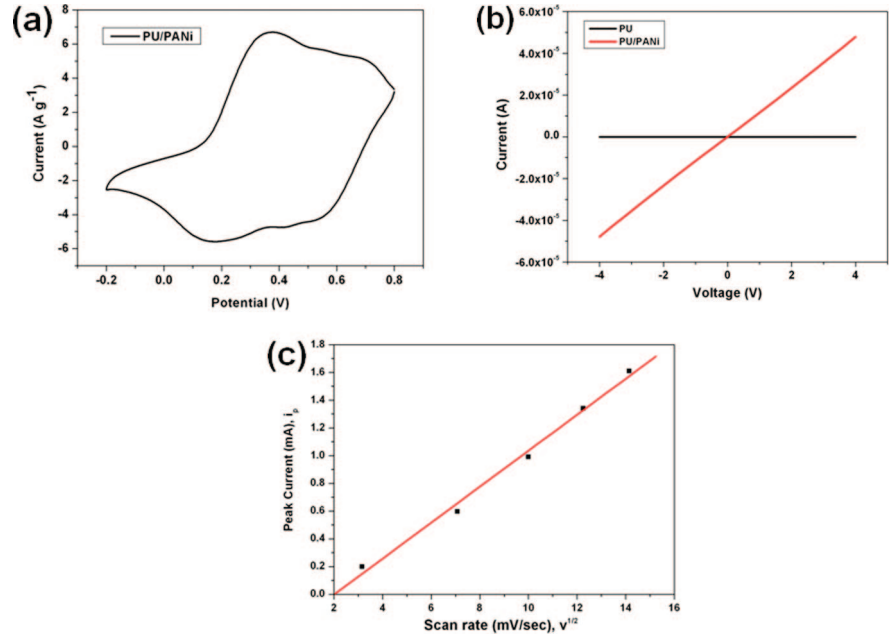

Figure 3. Characterization of conducting hybrid nanofibrous bundle. (a) Cyclic voltammogram of PU/PANi hybrid nanofibrous bundle in aqueous 1 M MSA solutions (scan rate = 5 mV/s). (b) $I-V$ characteristics of the pure PU and PU/PANi hybrid nanofibrous bundle. (c) Plot of diffusion coefficients of PU/PANi hybrid nanofibrous bundle at different scan rate.

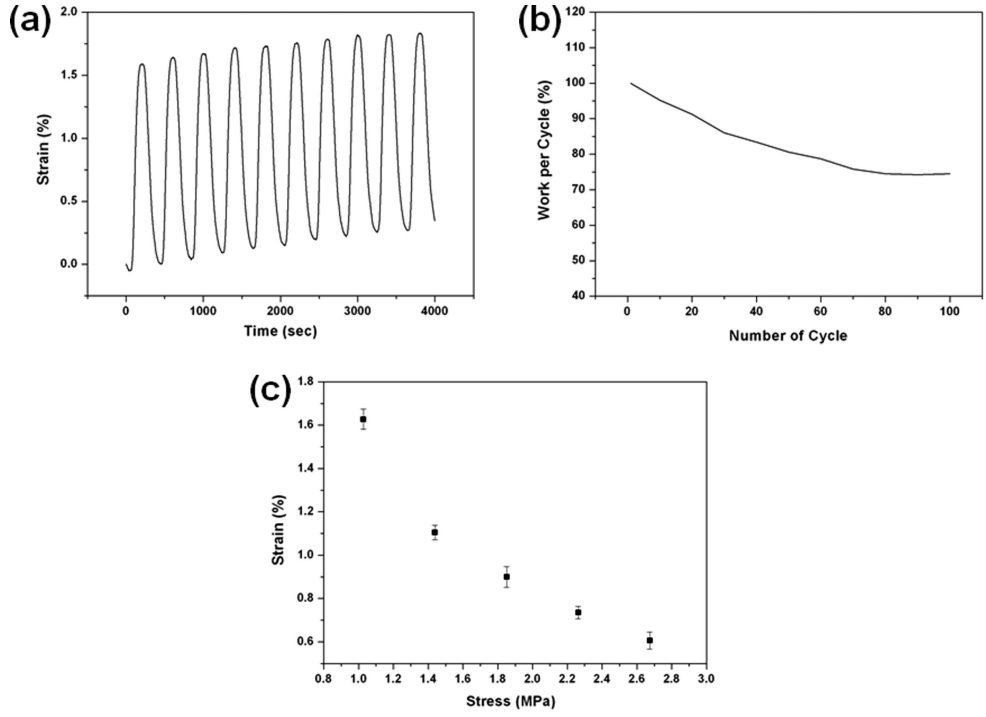

Figure 4. Actuation characteristics of PU/PANi hybrid nanofibrous bundle. (a) Electrochemical actuation profile upon cycling the potential between −0.2 to 0.8 V in aqueous 1 M MSA (scan rate = 5 mV/s, stress = 1.028 MPa). (b) Work per cycle relating to the stability of PU/PANi hybrid nanofibrous bundle (Electrolyte = 1 M MSA, scan rate = 5 mV/s, potential vs Ag/AgCl). (c) Variation of electrochemical actuation strain with change in applied stress.

was followed by contraction that was due to expulsion of anions when potential was reversed.[22] The active PANi layer is somewhat restricted by the passive PU core and the actuation strain generated by the PANi can be estimated using the "rule of mixtures" approach, as previously described.[15] Given a volume fraction of ~80%, the PANi layer must produce an actuation strain of around 2%. This linear actuation strain is comparable to or larger than that reported for PANi films[12] and fibers.[15,23,24] The bulk PANi films and fiber actuators reported previously have conductivities considerably higher (100−1000 S/cm) than the PANi coatings prepared here (0.5 S/cm). The similar actuation performance suggests that the thin PANi coating thickness and the nanoporous structure of the bundle facilitates larger actuation and compensates for the reduction in conductivity.

We also observed that the actuation of PU/PANi hybrid nanofibrous bundle was very stable up to 100 cycles (see Figure S3 in the Supporting Information). The actuation strain (ε_i) normalized to the strain produced in the first cycle (ε_0) is presented in Figure 4b. We observed that the biomimetic artificial nanofibrous bundle showed a stability of above 75% even beyond 100 cycles using a scan rate of 5 mV/s. The electrochemical actuation performances at different applied stress were also investigated and results are presented in Figure 4c. The actuation profiles are shown in the Supporting Information, Figure S4. The PU/PANi nanofibrous bundle shows negligible creep up to 11 mN load (2.3 MPa), above which it shows significant creep behavior in actuation. The isotonic actuation strain decreases with increasing external load as reported earlier for conducting polymer actuators.[15]

The fact that the PU/PANi hybrid nanofibrous bundle exhibited excellent mechanical stability suggested that the in situ chemical polymerization process did not affect the mechanical strength of PU nanofibers. Stress−strain curves of the PU/PANi nanofibrous bundle showed that the fiber could withstand stress over 30 MPa and broke when the load was exceeded 35 MPa (see Figure S5 in the Supporting Information). The bare PU nanofibers failed at around 25 MPa and a similar extension.

Another interesting feature observed in the nanofibrous bundle is its pseudocapacitive behavior. The capacitance value is calculated by integrating the CV loop corresponding to 116.24 F/g (see Figure S2 in Supporting Information). Faradaic reactions occurring at the surface of the nanofibrous bundles produces the pseudocapacitance behavior. The speed of these processes is enhanced by a large electrode/electrolyte interfacial area produced by the nanostructured PANi on the surface of individual nanofibers. The value is comparable with the previously reported surface grown nanostructured PANi systems.[25,26]

Conclusions

In conclusion, we have fabricated artificial myofibrils consisting of parallel electroactive nanofiber bundles. Mechanically robust but flexible nanofibrous polyurethane bundles were produced through electrospinning. These fibers were used as a template for controlled in situ chemical polymerization with aniline. The resulting PU/PANi nanofibrous bundle showed reasonably high electrical conductivity and responded to electrical stimuli generating a high linear actuation strain in aqueous electrolyte. The high surface area provided by nanostructured PANi on the individual nanofibers along with the high porosity allowed efficient incorporation of ions from the electrolyte leading to high strain and high charge storage capacity.

Acknowledgment. This work was supported by the Creative Research Initiative Center for Bio-Artificial Muscle of the Ministry of Education, Science and Technology (MEST)/the Korea Science and Engineering Foundation (KOSEF) in Korea.

Supporting Information Available: Additional figures and information (PDF). This material is available free of charge via the Internet at http://pubs.acs.org.

CM802377D

(22) Smela, E.; Mattes, B. R. *Synth. Met.* **2005**, *151*, 43.
(23) Lu, W.; Fadeev, A. G.; Qi, B.; Smela, E.; Mattes, B. R.; Ding, J.; Spinks, G. M.; Mazurkiewicz, J.; Zhou, D.; Wallace, G. G.; MacFarlane, D. R.; Forsyth, S. A. *Science* **2002**, *297*, 983.
(24) Mottaghitalab, V.; Xi, B. B.; Spinks, G. G.; Wallace, G. G. *Synth. Met.* **2006**, *156*, 983.
(25) Jang, J.; Bae, J.; Choi, M.; Yoon, S. H. *Carbon* **2005**, *43*, 2730.
(26) Wang, Y. G.; Li, H. Q.; Xia, Y. Y. *Adv. Mater.* **2006**, *18*, 2619.